Correlation between Nuclear Motion in the Core-Excited CF_4 Molecule and Molecular Dissociation after Resonant Auger Decay

K. Ueda,[1,2] M. Simon,[2,3] C. Miron,[2,3] N. Leclercq,[2,3] R. Guillemin,[2,3] P. Morin,[2,3] and S. Tanaka[4]
[1]*Research Institute for Scientific Measurements, Tohoku University, Sendai 980-8577, Japan*
[2]*LURE, Bat 209d, Universite Paris-Sud, 91405 Orsay Cedex, France*
[3]*CEA/DRECAM/SPAM, CEN Saclay, 91191 Gif/Yvette Cedex, France*
[4]*CIAS, Osaka Prefecture University, Sakai 599-8231, Japan*
(Received 7 April 1999)

Dissociation of the CF_4^+ molecular ion has been investigated using monochromatized synchrotron radiation and the energy-selected electron–ion coincidence method. The $2t_2^{-1}$ C ionic state produces fragment ions CF_2^+ and CF_3^+. The branching ratio CF_2^+/CF_3^+ is increased by a factor of ~ 6 by the C $1s$ excitation to the lowest unoccupied antibonding orbital, from the ratio at the direct ionization of the $2t_2^{-1}$ orbital. This increase is interpreted in the light of the nuclear motion in the core-excited state, with the help of theoretical calculations based on the vibronic model.

PACS numbers: 33.80.Gj, 33.15.Mt, 33.20.Rm, 33.80.Eh

Recent developments of the synchrotron radiation light sources and related beam line techniques allow one to excite any core electron to a specific quantum state using a narrow-band soft x-ray beam and to investigate the relaxation dynamics of the core-excited state in detail. Extensive observations of the resonant Auger processes and their theoretical analyses have revealed that the significant nuclear motion can take place within the lifetime of the core-excited states in some diatomic molecules [1–4]. Extensive observations of the ionic fragmentation of core-excited polyatomic molecules, on the other hand, revealed that the change of the molecular structure can take place in the core-excited states [5–8]. These findings enforce us to give up the conventional idea that the molecular dissociation starts at the Auger final state where the Auger transition is terminated and motivate us to examine the effect of the nuclear motion in the core-excited state on the molecular dissociation, i.e., the nuclear motion in the Auger final state.

It is known that there are two types of Auger decay processes following resonant core excitation to a discrete unoccupied molecular orbital. The first one is a participator Auger decay process, in which the excited electron participates in the decay. Its final state has one hole in the valence orbital and is thus identical to the final state of the direct valence photoionization, and thus one can observe the participator Auger process as the resonant enhancement of the valence photoemission line. The second one is a spectator Auger decay process, in which the excited electron behaves as a spectator in the decay process. Its final state has two holes in the valence orbitals and one electron in the excited orbital, and thus the energy of the spectator Auger final state is higher than that of the participator Auger final state. Therefore one can observe the spectator Auger band at lower energy than the resonant enhanced valence photoemission, i.e., the participator Auger band.

Characteristic features of the molecular dissociation caused by the core excitation mainly stem from the dissociative features of the spectator Auger final states and indeed most of the previous studies probed the molecular fragmentation via the spectator Auger decay [5–9]. The best way to extract a pure effect of the nuclear motion in the core-excited state on the molecular dissociation, however, is to compare the results of the molecular dissociation via the participator Auger decay (autoionization) with those via the direct valence photoionization, probing the same intermediate electronic state of the parent ion by use of the energy-selected electron-ion coincidence.

In this Letter, we carry out such coincidence experiments and in this way show the first clear evidence of an enhanced dissociation process of a molecular ion by the nuclear motion in the core-excited state. For this purpose, we use the C $1s$ excitation of a CF_4 molecule to the antibonding orbital often labeled as σ^*. We also present the results of the electron spectroscopy for the participator Auger decay and their theoretical analysis, in order to elucidate the dynamics of the nuclear motion in the core-excited state.

A CF_4 molecule is considered to be a suitable system for the present purpose because of the following reasons. (i) A large nuclear motion is expected in the C $1s^{-1}\sigma^*$ core-excited state because the C $1s$ core hole lifetime is long (~ 10 fs), and the coupling between the electron and the nuclear motion is expected to be strong in the C $1s^{-1}\sigma^*$ core-excited state as suggested by the broad width of the C $1s \rightarrow \sigma^*$ resonance (see [10] and Fig. 1). (ii) Molecular dissociation following the direct valence photoionization has been investigated extensively (see [11] and references cited therein) and thus we have a relatively solid basis to extract the effect of the nuclear motion in the core-excited state on the dissociation, by comparing the results following the participator Auger decay with those following the direct valence photoionization.

 0031-9007/99/83(19)/3800(4)$15.00

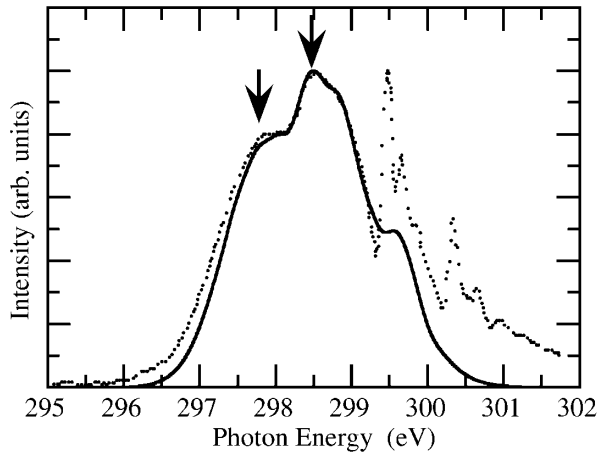

FIG. 1. The C 1s absorption spectra of CF_4. Dotted line, the experimental spectrum (from [10]). Solid line, the theoretical spectrum (present Letter).

The ground state electronic configuration of a CF_4 molecule which belongs to a T_d point group in its ground state is

$$\text{(core)}\ 1a_1^2\ 1t_2^6\ 2a_1^2\ 2t_2^6\ 1e^4\ 3t_2^6\ 1t_1^6; 4t_2^0\ 3a_1^0 \qquad (1)$$

where "(core)" includes F 1s and C 1s, $1a_1$ and $1t_2$ are mostly F 2s-like innervalence orbitals, $2a_1$ and $2t_2$ have C-F bonding character, and $1e$, $3t_2$, and $1t_1$ are mostly F 2p-like weakly bonding ($1e$ and $3t_2$) or nonbonding ($1t_1$) orbitals. In the present experiment, the C 1s core electron is excited into an unoccupied molecular orbital σ^*. In the C 1s absorption spectrum of CF_4 shown in Fig. 1, the broad band below 299 eV is attributed to this C $1s \rightarrow \sigma^*$ excitation [10,12,13]. The σ^* orbital in fact consists of the four equivalent antibonding orbitals made from the C sp^3 hybridized orbitals and the F 2p orbitals. These four orbitals are classified into the $4t_2$ and $3a_1$ irreducible representations in T_d symmetry. The broad width of the C $1s \rightarrow \sigma^*$ resonance suggests that large molecular deformation occurs when the C 1s core electron is excited to one of these antibonding orbitals in such a way that the bond corresponding to this excited orbital is elongated.

The experiment has been carried out using the plane-grating monochromator installed in the SA22 beam line at LURE in France. The bandpass of the monochromator was set to 0.1 eV at a photon energy of ~300 eV. The experimental setup combines a new high luminosity electron analyzer of double toroidal type with a conventional time-of-flight mass spectrometer. Full details of its design and operation were described elsewhere [14]. The measurements have been performed at the electron pass energy of 80 eV, resulting in 1-eV electron energy resolution. In order to preserve this resolution during the electron-ion coincidence measurement, a 1-kV pulsed extraction field is used.

The electron emission spectra were recorded at the C $1s \rightarrow \sigma^*$ resonance at the excitation energies given by arrows in Fig. 1. The two peaks in the spectra in Fig. 2 correspond to the emissions from the $2t_2$ and $3t_2$ valence orbitals. The direct photoemission spectrum from these orbitals is also given in Fig. 2 for comparison. It is clear from the figure that the intensity of these photoemission peaks is strongly enhanced by the C $1s \rightarrow \sigma^*$ excitation. This resonance enhancement corresponds to the participator Auger decay. The electron emission corresponding to the spectator Auger decay appears at kinetic energies below 270 eV and is not shown in the figure. The resonance-enhanced $2t_2$ peak has a long tail towards the lower kinetic energy side, and its position shifts linearly as a function of the photon energy (*dispersive effect* [15,16]). On the other hand, the resonance enhanced $3t_2$ peak does not have a tail and the position does not depend on the photon energy (*nondispersive effect* [15,16]). Such dispersive and nondispersive effects were observed by Ueda *et al.* [10] and Neeb *et al.* [17].

We now show our main results: the ion mass spectra taken in coincidence with the $3t_2$ and $2t_2$ photoemission lines in Fig. 2 are shown in Fig. 3, where the incident photon energies are 295 (off resonance), 297.7, and 298.5 eV (arrows in Fig. 1). The coincidence spectra issued from the $3t_2$ line show that the CF_4 molecule dissociates to CF_3^+ and F, and that this dissociation pattern is not affected by the C $1s \rightarrow \sigma^*$ excitation. On the contrary, the coincidence spectra issued from the $2t_2$ line shows that the $2t_2^{-1}$ C ionic state produces both CF_2^+ and CF_3^+ and that the C $1s \rightarrow \sigma^*$ excitation causes the increase of the branching ratio CF_2^+/CF_3^+ from the ratio at the direct ionization at 295 eV: the effect is more pronounced when the excitation is at the low energy side of the resonance. This is evidence that the dissociation

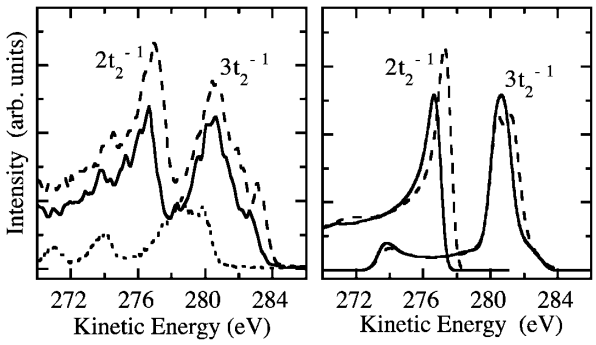

FIG. 2. The observed (left) and calculated (right) electron emission intensities, plotted as a function of electron kinetic energy. The two peaks correspond to the electron emissions from the $3t_2$ and $2t_2$ orbitals. The dashed and solid spectra were recorded at photon energies 297.7 and 298.5 eV, respectively, as indicated in Fig. 1 by arrows. The direct photoemission from the $3t_2$ and $2t_2$ orbitals at the photon energy 295 eV is given by the dotted line in the experimental spectrum for comparison.

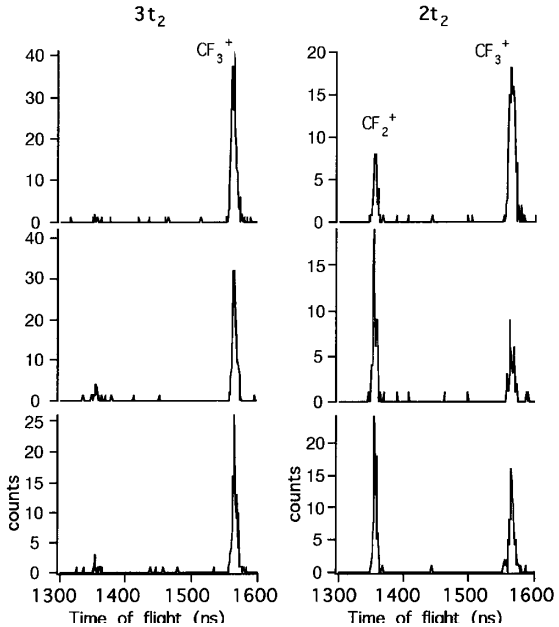

FIG. 3. Ion time-of-flight mass spectra taken in coincidence with the $3t_2$ (left) and $2t_2$ (right) electron lines, at 295 eV (top), 297.7 eV (middle), and 298.5 eV (bottom).

to CF_2^+ is induced effectively by the core excitation and thus we may call it *core-excitation-induced dissociation*.

It has been well established (see, e.g., [11] and references therein) that there are two decay channels from the $2t_2^{-1}$ C ionic state created by the direct photoionization: one is a radiative decay to the $3t_2^{-1}$ A and $1t_1^{-1}$ X states from which the CF_4^+ ion dissociates to $CF_3^+ + F$, and the other is predissociation to $CF_2^+ + F_2$. Because the latter dissociation process is as slow as the radiative process with a ns time scale, the existence of a potential barrier which distinguishes the $2t_2^{-1}$ C ionic state from the dissociation state $CF_2^+ + F_2$ was proposed by Creasey *et al.* [11]. Therefore, our result suggests that the nuclear motion in the core-excited state assists to induce the nuclear motion corresponding to the dissociation $CF_2^+ + F_2$ over the potential barrier in the Auger-final $2t_2^{-1}$ C ionic state.

In order to understand the mechanism of this core-excitation-induced dissociation, one needs to clarify the dynamics of the nuclear motion in the core-excited states. To do this, we conducted a theoretical investigation of the C $1s$ absorption and Auger emission spectra from a unified point of view. There are four independent molecular vibrations related to an elongation of the four equivalent C-F bonds under the C $1s \rightarrow \sigma^*$ excitation. These vibrational modes are classified into a symmetric stretching Q_{a_1} mode and an antisymmetric stretching Q_{t_2} mode in the T_d symmetry. We consider the Q_{t_2} mode as an interaction mode to be concerned here, because this mode gives rise to antisymmetric molecular deformation. Consequently, a linear coupling between the electron and the vibration of the Q_{t_2} mode causes the quasi-Jahn-Teller mixing between the C $1s^{-1}4t_2$ and the C $1s^{-1}3a_1'$ core-excited states in addition to the Jahn-Teller mixing within C $1s^{-1}4t_2$. Because the energy separations among these core-excited states are very small, the nonadiabatic transitions among these states are significant. Thus, we represent the Hamiltonian by the direct product basis of the electronic state and the number state of the vibration and diagonalize it by means of the Lanczos method to obtain the vibronic states. We also consider the Jahn-Teller coupling in the $3t_2^{-1}$ and $2t_2^{-1}$ Auger emission final states in the same way. The C $1s$ absorption and Auger emission spectra are calculated as first-order and as coherent second-order quantum processes, respectively. The parameters in the model are adjusted in order to reproduce the experiments satisfactorily. It should be noticed here that our model based upon a linear coupling and a harmonic approximation will be insufficient to illustrate the nuclear motion in the large Q range, where the mode-mode couplings might be important.

The adiabatic potentials for the core-excited states C $1s^{-1}\sigma^*$ are shown in Fig. 4 along $Q_{t_2x} + Q_{t_2y} + Q_{t_2z} \equiv Q_{[111]}$, the negative direction of which denotes the direction of the nuclear motion with a particular C-F bond elongated. The calculated adiabatic potentials along $Q_{[111]}$ for the $3t_2^{-1}$ A and $2t_2^{-1}$ C Auger final states are also shown in Fig. 4. Note that the CF_4 molecule belongs to the C_{3v} point group for $Q_{[111]} \neq 0$ and the T_2 degenerate states are split into A_1 and E symmetries. The $3t_2^{-1}$ ionic electronic state which is directly dissociative along $Q_{[111]}$ is well described by the A_1 curve in Fig. 4, showing a clear departure from the T_d symmetry. The $2t_2^{-1}$ state, which is not directly dissociative along the $Q_{[111]}$ coordinate, is not distorted along $Q_{[111]}$ and thus the two A_1 and E components for $Q_{[111]} \neq 0$ are identical along $Q_{[111]}$, as can be seen in Fig. 4. The core-excited $4t_2$ state is split into A_1 and

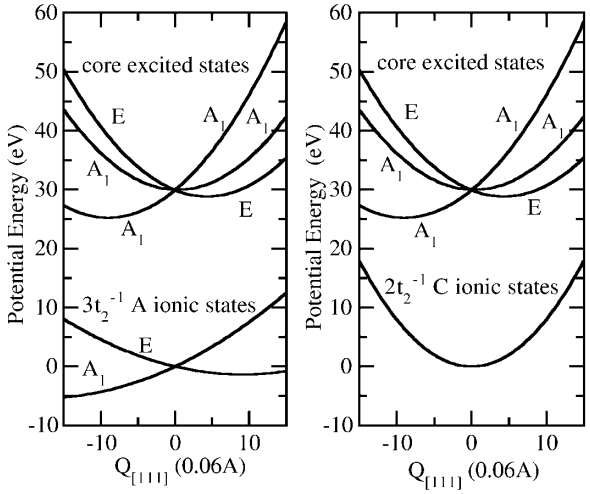

FIG. 4. The adiabatic potentials along $Q_{[111]}$ for the core-excited states C $1s^{-1}\sigma^*$ and for the final ionic states $3t_2^{-1}$ A and $2t_2^{-1}$ C of the Auger processes.

E components and, furthermore, the A_1 state couples with the nearly degenerate core-excited $3a_1A_1$ state at $Q_{[111]} \sim 0$. Thus the C $1s \rightarrow \sigma^*$ excitation corresponds to the overlap of the excitations to two A_1 states and one degenerate E state which are heavily coupled via nonadiabatic couplings. It is clear from Fig. 4 that the C-F bond is elongated (i.e., $Q_{[111]}$ becomes negative along the A_1 curve) upon the C $1s \rightarrow \sigma^*$ excitation.

The calculated C $1s$ absorption spectrum is compared with the experimental spectrum in Fig. 1. One can see that the calculated spectrum reproduces well not only the doublet structure but also the detailed fine structure in it. The calculated Auger emission spectra are compared with the experimental spectra in Fig. 2. The calculated spectra reproduce qualitatively the dispersive and nondispersive behaviors for the prominent peaks of the $2t_2$ and $3t_2$ lines, respectively, and the long low-energy tail of the $2t_2$ line. Since the core-excited state is common to both Auger emission processes, the difference of the spectral feature between them comes from the difference in stability between these two Auger-final states: the $2t_2^{-1}$ state is stable against Q_{t_2} while the $3t_2^{-1}$ state is unstable. This characteristic difference in the stability against the molecular deformation is clearly reflected in the photoemission spectrum [18].

Now we consider the $2t_2$ Auger emission spectrum. The Auger electron is emitted while the nuclear motion is going on in the core-excited states. As the nuclear motion proceeds, a part of the electronic excitation energy is converted to a vibration kinetic energy. According to the Franck-Condon principle, the Auger electron energy can be estimated from the energy difference in the potentials between the core-excited state and the Auger-final state, i.e., the Franck-Condon energy at a fixed Q. Since the nuclear motion starts at $Q_{t_2} \sim 0$ immediately after the photoexcitation and proceeds toward the negative direction of $Q_{[111]}$, the instantaneous Franck-Condon energy (i.e., the Auger electron energy) decreases with time as can be seen from Fig. 4. This energy decrease is the origin of the low-energy tail of the spectrum. On the other hand, the prominent peak is attributed to the prompt decay after the photoexcitation at $Q_{t_2} \sim 0$, where no vibration is excited, so the Auger electron energy linearly shifts with the incident photon energy.

We consider that the energy needed for CF_4^+ in $2t_2^{-1}$ C to go beyond the potential barrier to the $CF_2^+ + F_2$ dissociation channel is supplied by a conversion of the electronic excitation energy to the t_2-mode vibrational energy (i.e., nuclear-motion energy for the elongation of one particular C-F bond) in the core-excited state. The large amplitude of the oscillation in the final state thus created will cause the excitation of the other modes by a mode-mode coupling or higher-order interactions beyond the linear couplings, which will then lead to the $CF_2^+ + F_2$ dissociation channel. Moreover, it is clear from Fig. 4 that, on the low-energy side of the resonance, one preferentially excites the vibrational quanta in the A_1 electronic state, leading to an enhanced C-F elongation. At higher photon energy, one excites also other electronic states, with the Flanck-Condon factor in favor of low vibrational quanta because the potential curves are closer to the initial state. Consequently, a stronger dissociation of the molecule can be expected at low photon energy than at high photon energy, illustrating the observed change in the branching ratio to the CF_2^+ production along the resonance.

In contrast to the $2t_2$ Auger emission spectrum, the $3t_2$ Auger emission spectrum does not show a long tail. This is because the potential surfaces of the core-excited state and the $3t_2^{-1}$ A state are almost parallel and the $3t_2^{-1}$ A state is unstable against the Q_{t_2} mode as in the case of the core-excited states. As a result, the CF_3^+ fragment is produced together with the neutral F atom, irrespective to whether the $3t_2^{-1}$ A state is produced via Auger decay or via direct ionization.

In conclusion, dissociation to CF_2^+ from the CF_4^+ $2t_2^{-1}$ C state is enhanced by the core excitation. Though this dissociation does not occur in the core-excited state (note that the fragment CF_2^+ is not detected in coincidence with the $3t_2^{-1}$ Auger electrons), the nuclear motion along the Q_{t_2} vibration coordinate is induced in the core-excited state. This nuclear motion energy is transferred to the CF_4^+ $2t_2^{-1}$ C state via the Auger decay and stored as the t_2 vibrational energy, which is then transferred to the other modes and induces intramolecular reactions which leads to dissociation to CF_2^+ and F_2. We believe this is the first observation of the *core-excitation-induced* dissociation.

[1] P. Morin and I. Nenner, Phys. Rev. Lett. **56**, 1913 (1986).
[2] M. Neeb *et al.*, J. Electron. Spectrosc. Relat. Phenom. **67**, 261 (1994).
[3] F. Gelmukhanov and H. Ågren, Phys. Rev. A **54**, 379 (1996).
[4] O. Björneholm *et al.*, Phys. Rev. Lett. **79**, 3150 (1997), and references therein.
[5] T. LeBrun *et al.*, J. Chem. Phys. **98**, 2534 (1993).
[6] J. Adachi *et al.*, J. Chem. Phys. **102**, 7369 (1995).
[7] M. Simon *et al.*, Chem. Phys. Lett. **238**, 42 (1995).
[8] K. Ueda *et al.*, Phys. Rev. A **52**, R1815 (1995).
[9] K. Ueda *et al.*, Phys. Rev. A **46**, R5 (1992).
[10] K. Ueda *et al.*, J. Electron. Spectrosc. Relat. Phenom. **79**, 441 (1996).
[11] J. C. Creasey *et al.*, Chem. Phys. **174**, 441 (1993).
[12] J. A. Stephens *et al.*, J. Chem. Phys. **84**, 3638 (1986).
[13] W. Zhang *et al.*, Chem. Phys. **137**, 391 (1989).
[14] C. Miron *et al.*, Rev. Sci. Instrum. **68**, 3728 (1997).
[15] M. Simon *et al.*, Phys. Rev. Lett. **79**, 3857 (1997).
[16] S. Tanaka *et al.*, Phys. Rev. A **57**, 3437 (1998).
[17] M. Neeb *et al.*, J. Phys. B **30**, 93 (1997).
[18] A. J. Yencha *et al.*, J. Electron. Spectrosc. Relat. Phenom. **70**, 29 (1994).